J Geodesy (2007) 81:111–120
DOI 10.1007/s00190-006-0093-1

ORIGINAL ARTICLE

Calibration errors on experimental slant total electron content (TEC) determined with GPS

L. Ciraolo · F. Azpilicueta · C. Brunini · A. Meza · S. M. Radicella

Received: 9 November 2005 / Accepted: 12 August 2006 / Published online: 14 September 2006

Abstract The Global Positioning System (GPS) has become a powerful tool for ionospheric studies. In addition, ionospheric corrections are necessary for the augmentation systems required for Global Navigation Satellite Systems (GNSS) use. Dual-frequency carrier-phase and code-delay GPS observations are combined to obtain ionospheric observables related to the slant total electron content (sTEC) along the satellite-receiver line-of-sight (LoS). This observable is affected by inter-frequency biases [IFB; often called differential code biases (DCB)] due to the transmitting and the receiving hardware. These biases must be estimated and eliminated from the data in order to calibrate the experimental sTEC obtained from GPS observations. Based on the analysis of single differences of the ionospheric observations obtained from pairs of co-located dual-frequency GPS receivers, this research addresses two major issues: (1) assessing the errors translated from the code-delay to the carrier-phase ionospheric observable by the so-called levelling process, applied to reduce carrier-phase ambiguities from the data; and (2) assessing the short-term stability of receiver IFB. The conclusions achieved are: (1) the levelled carrier-phase ionospheric observable is affected by a systematic error, produced by code-delay multi-path through the levelling procedure; and (2) receiver IFB may experience significant changes during 1 day. The magnitude of both effects depends on the receiver/antenna configuration. Levelling errors found in this research vary from 1.4 total electron content units (TECU) to 5.3 TECU. In addition, intra-day variations of code-delay receiver IFB ranging from 1.4 to 8.8 TECU were detected.

Keywords Total electron content (TEC) · GPS, Inter-frequency bias · Differential code bias (DCB) · Levelling carrier to code TEC

L. Ciraolo
Istituto di Fisica Applicata "Carrara" del Consiglio Nazionale delle Ricerche (IFAC-CNR), ViaMadonna del Piano n. 10, 50019 Sesto Fiorentino (FI), Italy
e-mail: l.ciraolo@ifac.cnr.it

F. Azpilicueta (✉) · C. Brunini · A. Meza
Facultad de Ciencias Astronómicas y Geofísicas, Universidad Nacional de La Plata, Paseo del Bosque, 1900 La Plata, Argentina
e-mail: azpi@fcaglp.unlp.edu.ar

C. Brunini
e-mail: claudio@fcaglp.unlp.edu.ar

A. Meza
e-mail: ameza@fcaglp.unlp.edu.ar

C. Brunini · A. Meza
Consejo Nacional de Investigaciones Científicas y Tecnológicas, Argentina

S. M. Radicella
Aeronomy and Radiopropagation Laboratory, Abdus Salam International Centre for Theoretical Physics, Strada Costiera 11, 34014 Trieste, Italy
e-mail: rsandro@ictp.trieste.it

1 Introduction

The Global Positioning System (GPS) has become a tool that is routinely used to investigate the Earth's ionosphere (e.g., Schaer 1999, Hernandez-Pajares 2004). An important contribution to ionospheric studies based on Global Navigation Satellite Systems (GNSS) has been done by the International GNSS Service (IGS) (Beutler et al. 1999). Throughout the last decade, the IGS has supported a worldwide effort to deploy and maintain

operational a global network of GNSS receivers, whose observations were used by many scientists for a great variety of ionospheric studies (e.g., Gao et L. 1994, Feltens 1998, Mannucci et al. 1998, Hernández-Pajares et al. 1999, Schaer 1999). In addition, IGS established an Ionospheric Working Group in 1998 (Hernandez-Pajares 2004) that plays an important role in promoting and coordinating ionospheric studies based on GNSS observations.

The information retrieved from GNSS observations is the 3D (time, longitude and latitude) distribution of the vertical total electron content (TEC) (e.g., Brunini et al. 2004, Azpilicueta et al. 2005). TEC is defined as the integral of the electron density along a trajectory, usually, the vertical from the Earth's surface up to a given height in the ionosphere (hence, vertical or vTEC) or the line-of-sight (LoS) from the satellite to the receiver (slant or sTEC). TEC is measured in TEC units (TECU), with 1 TECU being 10^{16} electrons/m^2.

The ionospheric delay constitutes the main source of error for single-frequency GNSS operation. The sensitivity of the ionospheric range delay to sTEC for the primary GPS signal is 0.162 m per TECU. Hence, the range delay for this signal can reach as much as 90 m for a low-elevation satellite (e.g., Langley 1996). An application of ionospheric models is found in the so-called augmentation systems, which encompass a variety of services developed to provide the single-frequency GPS user (particularly in civilian aviation) with corrections that attenuate the ionospheric and other navigational errors (Walter et al. 2004).

Examples of operational or nearly operational services are the Wide Area Augmentation System (WAAS) in the USA and Canada (see http://gps.faa.gov/Programs/WAAS/waas.htm), the European Geostationary Navigation Overlay System (EGNOS) (see http://www.esa.int/esaNA/egnos.html/) and the Multifunctional Transport Satellite Space Based Augmentation System (MSAS) in Japan (see http://directory.eoportal.org/pres_MTSATMultifunctionTransportSatellite.html). The necessity of extending such services to other regions of the world with different ionospheric conditions (Central and South America, Africa, India, China, etc.) has raised the interest of many scientists on GNSS-based ionospheric models.

To a good approximation, the refractivity of the ionospheric plasma for GNSS signals is directly proportional to the electron density and inversely proportional to the square of the signal frequency. Brunner and Gu (1991) and Bassiri and Hajj (1992) reported that the errors introduced when using this approximation instead of the complete Appleton–Hartree formula is of the order of a few centimetres. Based on this approximation, the subtraction of simultaneous observations made at different frequencies allows us to obtain an ionospheric observable related to the satellite-receiver sTEC (e.g., Leitinger and Putz 1988). This ionospheric observable can be obtained from either carrier-phase or code-delay measurements.

Carrier-phase observations are much less affected by measurement noise and multi-path than code-delay observations, but they present the additional problem of being biased by unknown ambiguities (e.g., Mannucci et al. 1998). A widely used procedure to reduce the ambiguities from the carrier-phase ionospheric observable is the so-called "levelling carrier to code" algorithm (see Sect. 2). One objective of this paper is to investigate the presence of systematic errors in the levelled carrier-phase ionospheric observable caused by the use of this algorithm.

Early investigations concerning sTEC determination with GPS pointed out the existence of systematic delays produced by both transmitter and receiver hardware (e.g., Lanyi and Roth 1988, Gaposchkin and Coster 1993, Sardon et al. 1994, Davies and Hartmann 1997). Because these delays are different from frequency to frequency (and from carrier-phase to code-delay observations), an IFB remains present in the ionospheric observable after subtracting observations at different frequencies. Code-delay IFBs are also called differential code biases (DCB) in the literature devoted to GPS-based TEC studies (e.g., Hernández-Pajares et al. 1999, Mannucci et al. 1998, Sardon et al. 1994).

Satellite and receiver IFBs combined might reach several tens of nanoseconds or, equivalently, 100 TECU; therefore, their effect has to be removed from the ionospheric observable in order to obtain unbiased sTEC estimates. To separate sTEC from IFB, the spatial and temporal variability of sTEC is represented by means of a variety of approaches (e.g., Ma et al. 2005, Brunini et al. 2003, Otsuka et al. 2002, Jakowsky et al. 1996), while IFB are assumed to be constant for a given period of time, usually 1–3 days (Bishop et al. 1994, Sardon and Zarraoa 1997, Brunini et al. 2005). A second objective of this paper is to assess the short-term temporal variability of receiver IFBs.

2 The ionospheric observable

The ionospheric observable has been discussed extensively in the literature (e.g., Mannucci et al. 1999 and references therein). It is obtained based on fact that the ionospheric effect on the GPS signals depends on the signal frequency f and on the sTEC between the satellite

and the receiver as:

$$I = \alpha \frac{\text{sTEC}}{f^2}, \quad (1)$$

where I is the ionospheric range delay at frequency f and α is a constant value used to convert from TECU to length units.

Hence, subtraction of simultaneous observations at different frequencies leads to an observable, L_I, in which all frequency-independent effects (e.g., the satellite-receiver geometrical range, clock errors, tropospheric delay, etc.) are cancelled, but the ionospheric and any other frequency-dependent effects remain:

$$L_{I,\text{arc}} = L_1 - L_2 = I_1 - I_2 + c(\tau_{R1} - \tau_{R2}) + c(\tau_{S1} - \tau_{S2}) + \frac{c}{f_1} N_{1,\text{arc}} - \frac{c}{f_2} N_{2,\text{arc}} + \varepsilon, \quad (2)$$

where the sub-indexes 1 and 2 refer to the GPS carriers L1 and L2 and sub-index "arc" refers to every continuous arc of carrier-phase observations (i.e., a group of consecutive observations along which the ambiguities on L1 and L2 do not change); c is the speed of light in vacuum; L_1 and L_2 are the carrier-phase measurements expressed in length units; I_1 and I_2 are the ionospheric delays in length units; τ_R and τ_S are frequency-dependent biases associated to delays produced by the receiver and the satellite hardware, respectively, expressed in time units; N_1 and N_2 are the integer carrier-phase ambiguities; and ϵ is the combination of observational noise and multi-path in L1 and L2 carrier-phase observations.

By using Eq. (1), Eq. (2) can be converted into

$$L_{I,\text{arc}} = \text{sTEC} + B_\text{R} + B_\text{S} + C_\text{arc} + \varepsilon_L, \quad (3)$$

where $L_{I,\text{arc}}$ is the ionospheric observable; $B_\text{R} = \frac{c}{\beta}(\tau_{\text{R}1} - \tau_{\text{R}2})$ and $B_\text{S} = \frac{c}{\beta}(\tau_{\text{S}1} - \tau_{\text{S}2})$ are the so-called satellite and receiver IFBs for the carrier-phase observations; $\beta = \alpha\left(\frac{1}{f_1^2} - \frac{1}{f_2^2}\right) \cong 0.1$ m/TECU is a constant value used to convert from metres to TECU; $C_\text{arc} = \frac{c}{\beta f_1} N_{1,\text{arc}} - \frac{c}{\beta f_2} N_{2,\text{arc}}$ is the bias produced by carrier-phase ambiguities in the ionospheric observable; and $\varepsilon_L = \frac{\varepsilon}{\beta}$ is the effect of noise and multi-path. All terms in Eq. (3) are expressed in TECU.

Using the dual-frequency, P, code-delay observations, an analogous ionospheric observable can be obtained

$$P_I = \text{sTEC} + b_\text{R} + b_\text{S} + \varepsilon_P, \quad (4)$$

where the meanings of the terms are analogous to Eq. (3) with the following differences: P_I is obtained by subtracting P_1 from P_2 (the ionospheric range delay for code-delay observations have opposite sign than for carrier-phase); b_R and b_S are the satellite and receiver code-delay IFBs, which are different from those for carrier-phase; there is not any ambiguity term for code-delay; and the effect of noise and multi-path for code-delay observations, ε_P, is around 100× greater than for carrier-phase observations (Braasch 1996). Multi-path effects occur when the direct signal coming from the satellite is mixed with those reflected from objects in the vicinity of the receiving antenna.

At this point, it is important to note that the terms L_I and P_I are the only terms derived from the direct measurements L_1, L_2, P_1 and P_2, while the other terms are either constants or parameters to be estimated.

Once the ionospheric observables have been obtained from carrier-phase and code-delay observations, the average of the differences between them is computed for every continuous arc thus obtaining $\langle L_I - P_I \rangle = {}^1\!/_N \sum_1^N (L_I - P_I)_i$, where N is the number of continuous measurements contained in the arc. Using Eqs. (3) and (4), and assuming constant IFBs, we found that:

$$\left\langle L_{I,\text{arc}} - P_I \right\rangle_\text{arc} = C_\text{arc} + B_\text{R} - b_\text{R} + B_\text{S} - b_\text{S} - \langle \varepsilon_P \rangle_\text{arc}, \quad (5)$$

It should be noted that Eq. (5) neglects the effect of noise and multi-path on carrier-phase observations, but this has no influence in the results since these effects are 100× smaller than the ones on the code-delay.

Subtracting Eq. (5) from (3), the ambiguity term is removed from the carrier-phase ionospheric observable

$$\tilde{L}_{I,\text{arc}} = L_{I,\text{arc}} - \left\langle L_{I,\text{arc}} - P_I \right\rangle_\text{arc} = \text{sTEC} + b_\text{R} + b_\text{S} + \langle \varepsilon_P \rangle_\text{arc} + \varepsilon_L \quad (6)$$

where $\tilde{L}_{I,\text{arc}}$ is the carrier-phase ionospheric observable 'levelled' to the code-delay ionospheric observable. This procedure is known as the 'carrier to code levelling process'.

Equation (6) shows that, after the levelling process: (1) the carrier-phase IFBs are replaced by the corresponding code-delay IFBs; and (2) the levelled carrier-phase ionospheric observable may be affected by noise and multi-path present in the code-delay observations, if these quantities do not average to zero over a continuous arc.

It is important to note that in deriving Eq. (6), the assumption mentioned in Sect. 1 about constant satellite and receiver IFB was applied. This issue and the non-zero average effects will be revised later in this paper.

3 Methodology

This section describes the procedure applied to assess the effects of systematic errors on the levelled carrier-phase ionospheric observable (Eq. 6). The investigation

is based on data from co-located GPS receivers. In this context, the word "co-located" is intended as two receivers separated one from the other by few metres, so that the sTEC can be considered equal for both receivers. Additional data from a dedicated experiment were analysed, which consisted of two identical GPS receivers connected to the same antenna through an antenna splitter. In this case, not only the measured sTEC but also the errors were the same for both receivers.

Single differences of data from the same satellite collected simultaneously by the two receivers, A and B (i.e., single differences of the ionospheric observable), yield to Eq. (7) for code-delay and Eq. (8) for carrier-phase levelled to code-delay observations.

$$\begin{aligned} \Delta P_I &= P_{I,A} - P_{I,B} = b_{\mathrm{R},A} - b_{\mathrm{R},B} + \varepsilon_{PA} - \varepsilon_{PB} \\ \Delta P_I &= \Delta b_{\mathrm{R}} + \Delta \varepsilon_P, \end{aligned} \tag{7}$$

$$\begin{aligned} \Delta \tilde{L}_{I,\mathrm{arc}} &= L_{I,\mathrm{arc},A} - L_{I,\mathrm{arc},B} = b_{\mathrm{R}A} - b_{\mathrm{R}B} \\ &\quad + \langle \varepsilon_P \rangle_{\mathrm{arc},A} - \langle \varepsilon_P \rangle_{\mathrm{arc},B} + \varepsilon_{LA} - \varepsilon_{LB} \\ \Delta \tilde{L}_{I,\mathrm{arc}} &= \Delta b_{\mathrm{R}} + \Delta \langle \varepsilon_P \rangle_{\mathrm{arc}} + \Delta \varepsilon_L \end{aligned} \tag{8}$$

where Δ is the "single difference" operator (sTEC and satellite IFB are cancelled by the single difference computation).

According to Eq. (8), single differences of the levelled carrier-phase ionospheric observable should be a constant independent of the observed satellite, Δb_{R}, defined as the difference of the IFB of the receivers. It is expected that the data belonging to different satellite arcs deviate from Δb_{R} by an arc-dependent quantity, $\Delta \langle \varepsilon_P \rangle_{\mathrm{arc}}$, because: (1) code-delay noise and multi-path effects may not be totally removed by the levelling process and (2) the remaining effect are different on both receivers. In addition, small fluctuations, $\Delta \varepsilon_L$, due to carrier-phase noise and multi-path, should be present in the single differences.

In order to present the results in the following sections, a rough estimate of the expected error $\Delta \langle \varepsilon_P \rangle_{\mathrm{arc}}$ in the single differences is necessary. Although this estimate is based on assumptions that are likely to be inadequate, it can be justified by the fact that these assumptions are the same as the one used in the calibration algorithm. In principle, it can be assumed that the error of a single-difference observation is $\sqrt{2}\times$ greater than the error of a levelled carrier-phase ionospheric observation, i.e., $\Delta \langle \varepsilon_P \rangle_{\mathrm{arc}} = \sqrt{2} \langle \varepsilon_P \rangle_{\mathrm{arc}}$. Following Eq. (6) the levelled carrier-phase ionospheric observable is affected by an arc-dependent error (hereafter named "levelling error"), $\langle \varepsilon_P \rangle_{\mathrm{arc}}$, equal to the average of the combined effect of code-delay multi-path and noise along a continuous arc.

If the carrier-phase observations are not affected by cycle slips, a continuous arc may last approximately 6 h and contain around 700 pairs (code-delay and carrier-phase) of observations, assuming a 30 s sampling interval (cycle slips and continuity of the arcs were checked following Blewitt 1990). Code-delay noise can be considered as a random 'signal', but code-delay multi-path should be treated as a systematic one. In spite of this, it will be assumed that the expectation value for the combined effect of code-delay multi-path and noise is equal to zero and its root mean square (RMS) error decreases with the inverse of the square root of the number of averaged samples.

According to Brunini (1998), the RMS error of code-delay ionospheric measurement increases exponentially as the satellite elevation decreases, from a fraction of TECU close to the zenith to approximately ± 10 TECU at an elevation of 10°. Assuming the worst case of ± 10 TECU and a set of 700 measurements, an error limit on the order of $\pm 10 / \sqrt{700}$ TECU ≈ 0.38 TECU is obtained. This means that $\Delta \langle \varepsilon_P \rangle_{\mathrm{arc}} \leqslant \sqrt{2}\, 0.38$, i.e., the expected error for the single differences should not be greater than a fraction of TECU.

The analysis that will be presented in Sect. 4 indicates the existence of levelling errors much greater than the optimistic "fraction of TECU". The explanation for this might be that the assumption of code-delay multi-path effect averaging to zero is not valid, as is suggested by Byun et al. (2002).

4 Results

Table 1 summarizes the relevant characteristics of the data set used in this research: four-character station name, receiver and antenna type, approximate longitude and latitude of the receivers and period of time covered by the observations. The receivers belong to the IGS (http://igscb.jpl.nasa.gov/) and to the EGNOS test bed (http://www.essp.be/) networks.

In addition, a dedicated experiment was performed at National University of La Plata (UNLP) with the aim to eliminate errors due to other sources than code-delay multi-path. It consisted of a "zero-baseline" experiment (i.e., two identical receivers, namely LPGB and LPGR, connected to the same antenna via an antenna splitter device). This zero-baseline antenna was set up very close (few metres) to the LPGS receiver (belonging to IGS) and to the LPG2 receiver [belonging to CHAllenging Mini-satellite Payload (CHAMP) mission managed by Germany's National Research Centre for Geosciences;

Table 1 Data sets used in this research

Station name	Organization	Receiver type	Antenna type	Longitude–latitude	Observation period
LPGS	IGS	(1118) AOA Benchmark ACT 3.3.32.2N	(367) AOAD/M_T	57.9°W, 34.9°S	2005, days 188–191
LPG2	CHAMP	(1135) AOA Benchmark ACT 3.3.32.2N	(508) AOAD/M_T		
LPGB	UNLP	NovAtel Millenium	NovAtel 503		
LPGR	UNLP	NovAtel Millenium			
POTM	CHAMP	(1106) AOA Benchmark ACT 3.3.32.2N	(346) AOAD/M_T	13.1°E, 52.4°N	2004, days 001–030
POTS	IGS	(281-U) AOA SNT-8000 ACT 3.3.32.3	(235) AOAD/M_T		
TLSE	IGS	(30708) TRIMBLE 4000SSI 7.19A	(227554) TRM29659.0	1.5° E, 43.6°N	2004, day 336; 2005, day 212
TLSM	EGNOS	(SLG9803) NovAtel Millenium 4.45	(CRG0xxx) ASH701073.1 S		

GeoForschungsZentrum (GFZ), Potsdam; http://www.gfz-potsdam.de/welcome_en.html].

4.1 Analysis of the levelled single differences of the carrier-phase ionospheric data

Figure 1 shows single differences of the levelled carrier-phase ionospheric observable (Eq. 8) for different pairs of co-located receivers and for different days (different satellites are represented with different colours). The sampling interval is 30 s and the cut-off elevation mask is 10°. Figure 1 shows representative cases of the different situations found in the analysis.

A first conclusion extracted from this analysis is that the levelling error, which is inferred from the spread between single differences corresponding to different arcs, is strongly dependent on the antenna/receiver configuration. The upper panels of Fig. 1 show the cases with the maximum differences found in the sample, both corresponding to the LPGB–LPGS combination. In these cases, the arc-to-arc spread reaches a peak-to-peak value of almost 15 TECU, which leads to a levelling error of $\frac{\left(15/\sqrt{2}\right)}{2} \approx 5.3$ TECU (a 95% significance was used to estimate the levelling errors).

Complementarily, the bottom panels of Fig. 1 show the cases with the minimum differences found in the sample, both corresponding to the LPGS–LPG2 combination (same receiver/antenna configuration). In these cases, the peak-to-peak spread is lower than 4 TECU, which leads to levelling errors of approximately 1.4 TECU. It should be noted, however, that the actual levelling error could be larger than this value, because an identical receiver/antenna configuration may introduce correlation between the errors of undifferenced data.

Another conclusion extracted from the analysis of the sample is that, for some days, single differences of levelled carrier-phase ionospheric data show an intra-day variation that affects all satellites and arcs in a magnitude that depends on the receiver/antenna configuration. This variation is truly apparent on day 188 for the LPGB–LPGS configuration (upper-left panel of Fig. 1), as an inverted "U-shape" with peak-to-peak range of almost 25 TECU. For the same day, a less pronounced variation with peak-to-peak range of about 4 TECU is also present for the LPGS–LPG2 configuration (bottom-left panel). On day 189, the variation is neither evident for LPGB–LPGS (upper-right panel) nor for LPGS–LPG2 (bottom-right panel) configurations.

Following Eq. (8) this variation could be attributed to instabilities of the code-delay IFBs, combined through the single difference operation in the term Δb_{R}. Then, assuming that the variations of both receivers are uncorrelated, receiver code-delay IFBs variations of $\frac{\left(25/\sqrt{2}\right)}{2} \approx 8.8$ TECU can be found in the LPGB–LPGS configuration and of $\frac{\left(4/\sqrt{2}\right)}{2} \approx 1.4$ TECU for the LPGS–LPG2 configuration.

In summary, two different processes have been discussed: (1) an arc-dependent systematic levelling error associated with effects that do not cancel after averaging the data for a continuous arc. These biases can be associated with code-delay multi-path effects and also with different measurement techniques (see Gao et al. 2001); and (2) an intra-day variation of the code-delay receiver IFB is present in some days' data and not others. Section 4.2 provides an insight into the issues mentioned above, using only code-delay observations. It is important to mention that the magnitude of both effects depends on the receiver/antenna configurations.

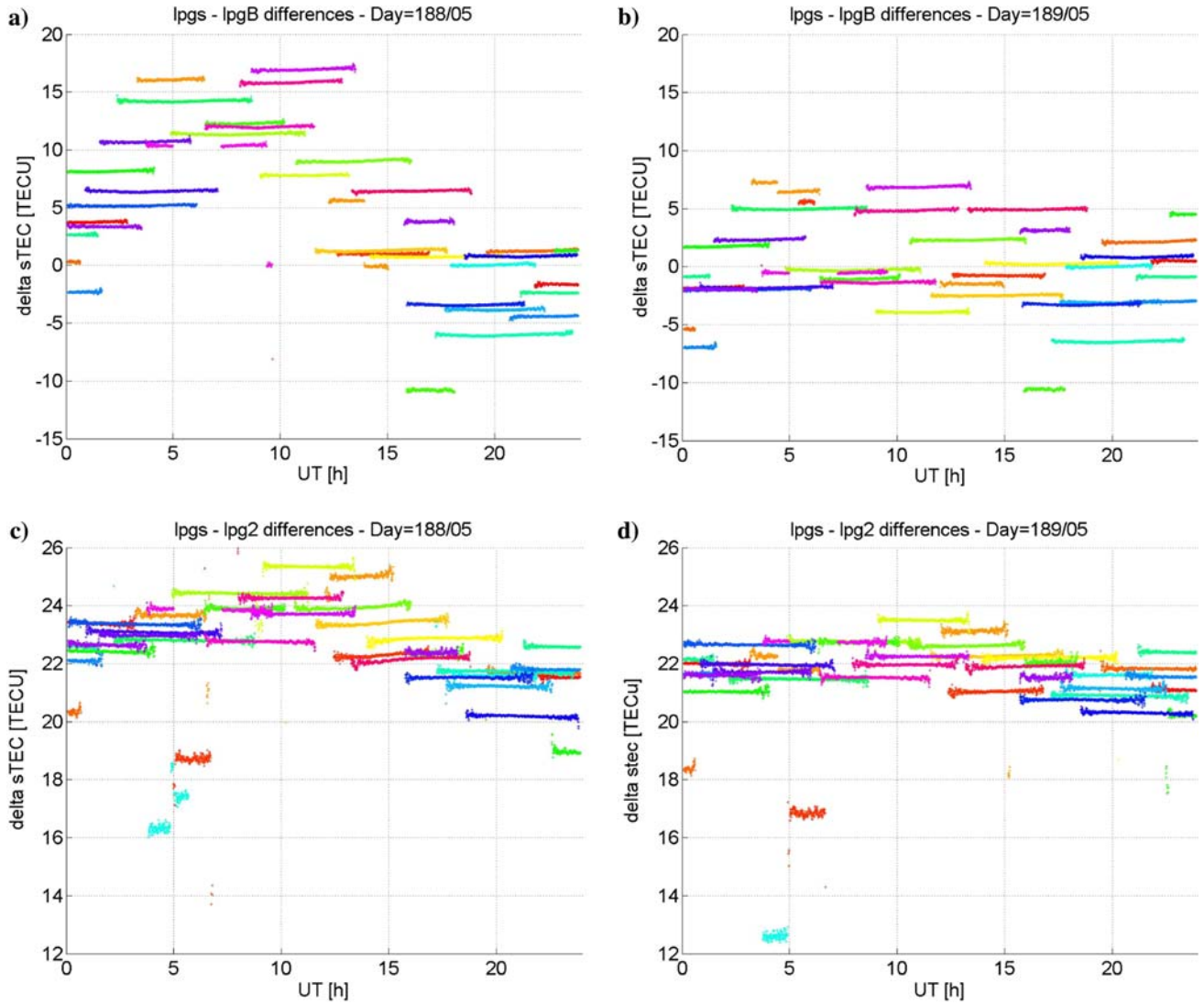

Fig. 1 Single differences of the levelled carrier-phase ionospheric observable (different *colours* correspond to different satellites). **a** Sites: lpgs and lpgB, day 188/05. **b** Sites: lpgs and lpgB, day 189/05. **c** Sites: lpgs and lpg2, day 188/05. **d** Sites: lpgs and lpg2, day 189/05

In order to get a closer approach to the effect of the receiver measure technique and the influence of the code-delay multi-path on the levelling procedure, single-differenced levelled carrier-delay ionospheric data from the zero-baseline experiment involving the LPGB and LPGR receivers are analysed. In this case, the zero-baseline experiment cancels the possible influence of multi-path, while the use of two identical receivers eliminates any difference due to the measurement technique.

Figure 2 shows the corresponding results for the same days previously shown in the upper panels of Fig. 1. As it was expected, the arc-to-arc spread has been significantly reduced up to a peak-to-peak value lower than 2 TECU. It is also noticeable that the temporal variation of code-delay receiver IFB present on day 188 for the LPGB–LPGS configuration (upper-left panel of Fig. 1) is also reduced (even if it does not disappear completely) in the zero-baseline experiment (left panel of Fig. 2).

4.2 Analysis of code-delay multi-path effect and the instabilities of the code-delay receiver IFB

From the analysis previously presented, it follows that the arc-to-arc spread and the intra-day variation of the levelled carrier-phase are associated with the present in code-delay observations that are introduced into the levelled carrier-phase observations by the levelling process. Thus, the origin of both problems should be traced back to code-delay rather than to carrier-phase data. The following analysis, based on the code-delay ionospheric observable (Eq. 7), instead of the levelled carrier-phase

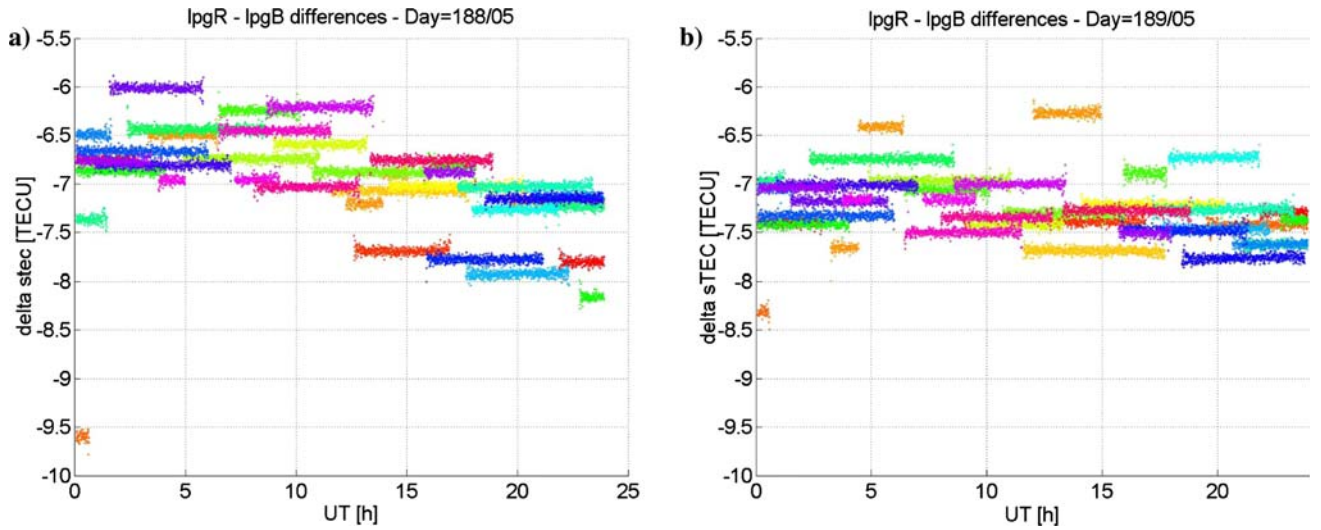

Fig. 2 Single differences of the levelled carrier-phase ionospheric observable (different *colours* correspond to different satellites). **a** Sites: lpgR and lpgB, day 188/05. **b** Sites: lpgR and lpgB, day 189/05

ionospheric observable (Eq. 8), is presented in order to confirm this assertion.

Figure 3 is analogue to Fig. 1, but obtained from smoothed code-delay data. The reason for data smoothing is to attenuate the effect of the large random noise that affects the code-delay ionospheric observations, thus recovering any underlying systematic signals. This was achieved by applying the following procedure: firstly, a cut-off elevation mask of 60° was imposed in order to discard low-elevation data; then, a low-pass filter was applied in order to reduce high-frequency effects of random noise. For the sake of simplicity, we have chosen a low-pass filter based on a moving average with a rectangular window.

The spectral analysis of the single difference signals for the co-located receivers and days shown in Fig. 3, presented peaks on the power spectrums at approximately 0.002 Hz. In order to preserve this signal, we adopted a window width of 4 min. Comparing Fig. 3 with Fig. 1 brings out that, though the scatter of the plots has largely increased, the relevant behaviour of Fig. 1 (i.e., the arc-to-arc spread and the intra-day variability) can be easily recognized in Fig. 3. This fact confirms the assertion about the code-delay origin of both the spread and the intra-day variability observed in the carrier-phase single differences.

Since the relative position of the GPS satellites, receiving antennas and objects that can produce signal reflections and diffractions repeats after one sidereal day, the multi-path effect is characterized by a pattern that repeats with one sidereal day period (e.g., Braasch 1996). If the levelling error is effectively produced by code-delay multi-path, the single-differences of the code-delay ionospheric observable for a given satellite should exhibit a systematic pattern shifted by approximately 4 min from one solar day to the next. This behaviour was effectively confirmed for all samples described in Table 1.

Figure 4 shows the results obtained for one particular satellite and for two particular pairs of co-located receivers (LPGB–LPGS and POTS–POTM). Each panel of Fig. 4a and b shows four lines: representing the single-differenced code-delay ionospheric observable corresponding to four consecutive days, represented against Universal Time (UT) (upper panel) – UT for the second, third and fourth days is corrected for the ∼4 min daily shift with respect to the first day; satellite azimuth (second panel); elevation angle for the ascending and descending satellite trace (third and fourth panels). The fingerprint of multi-path can easily be recognized. It does not make sense to show plots for other satellites or other co-located receiver pairs, because all of them lead to similar conclusions to those already reported here.

5 Conclusions

Code-delay GPS observations are biased by frequency-dependent systematic biases produced by both the satellites and the receiver. The difference of these biases leads to the introduction of a satellite and a receiver IFB in the code-delay ionospheric observable. These code-delay IFBs are later translated to the carrier-phase ionospheric observable, when carrier phase data are levelled to code-delay data in order to eliminate the carrier-phase ambiguities.

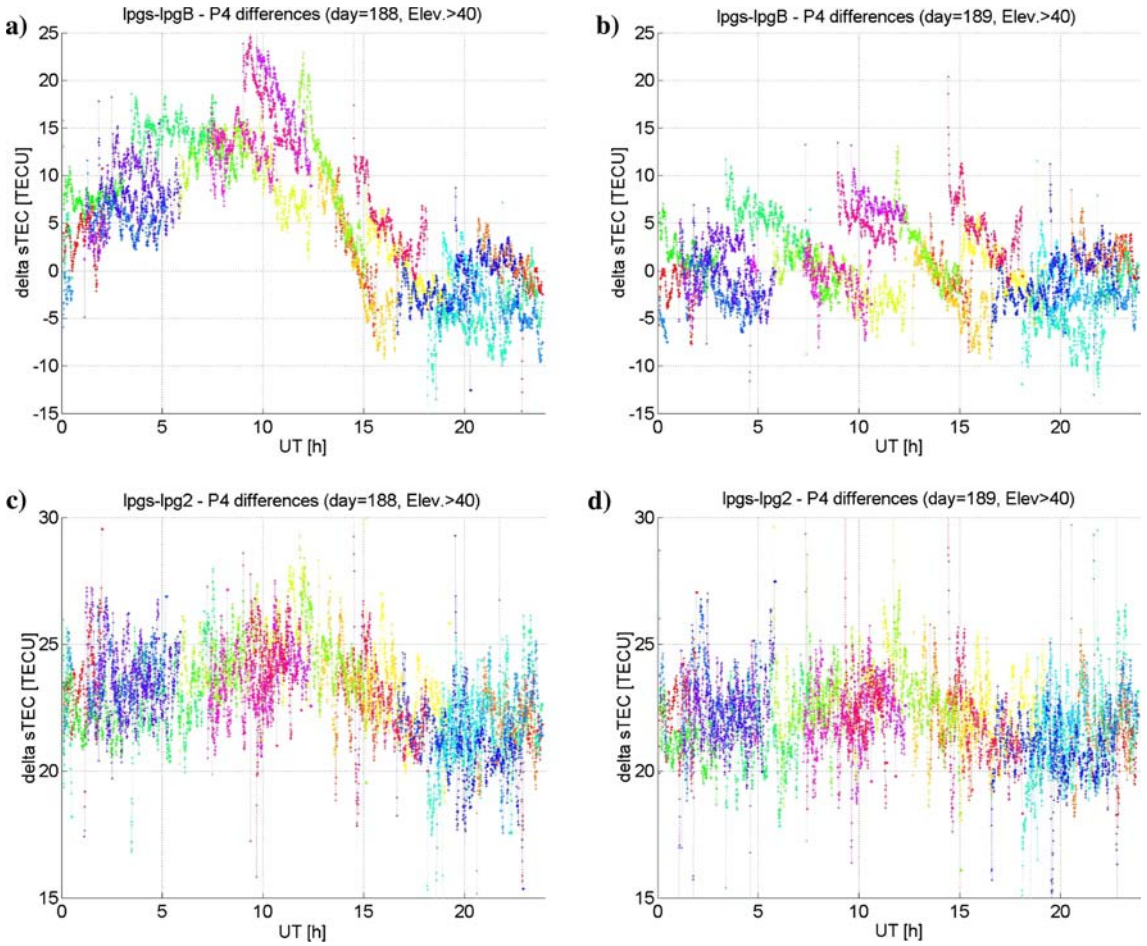

Fig. 3 Smoothed single differences of the code-delay ionospheric observable (different *colours* correspond to different satellites). **a** Sites: lpgs and lpgB, day 188/05. **b** Sites: lpgs and lpgB, day 189/05. **c** Sites: lpgs and lpg2, day 188/05. **d** Sites: lpgs and lpg2, day 189/05

Since the combination of satellite and receiver IFB may reach a value as large as 100 TECU, they should be estimated and eliminated from the data in order to obtain calibrated sTEC observations from GPS data. For calibration purposes, it is often assumed that both satellite and receiver code-delay IFBs are constant during 1–3 days (e.g., Sardon and Zarraoa 1997, Schaer 1999, Brunini et al. 2005). This research focussed on two major issues: (1) to assess the errors translated from the code-delay to the carrier-phase ionospheric observable by the levelling process; and (2) to assess the intra-day stability of code-delay receiver IFB. The research was based on the analysis of single-differences of ionospheric observations obtained from pairs of co-located GPS receivers. The main conclusions are summarized in the following paragraphs.

The levelled carrier-phase ionospheric observable is affected by systematic errors whose effects do not cancel after averaging all the data in a continuous arc. Different experiments were conducted with the aim to isolate the cause of these errors. The results obtained allow us to speculate that code-delay multi-path is the main contributor to levelling errors. Even for the same satellite, two different arcs are generally affected by different levelling errors. Hence, the code-delay ionospheric observable would be better modelled if an arc-dependent bias, $\tilde{b}_{\mathrm{arc}}$, is included in Eq. (4), instead of a receiver-dependent IFB, b_{R}. Such arc-dependent bias, $\tilde{b}_{\mathrm{arc}}$, should account for receiver-dependent IFB, b_{R}, and for the arc-dependent levelling error, $\langle \varepsilon_P \rangle_{\mathrm{arc}}$.

Code-delay receiver IFB can be affected by significant intra-day variations. Even for the case of the same receiver/antenna configuration, the pattern for the difference of the IFB for 1 day can be significantly different from the pattern for the following day. The cause of this could be associated with changes in the environmental conditions nearby the antenna/receiver.

The magnitude of both effects, levelling errors and intra-day variability of code-delay receiver IFB, is dependent on the receiver/antenna configuration. Levelling errors varying from 1.4 to 5.3 TECU were found in this research. Beside, intra-day variations of

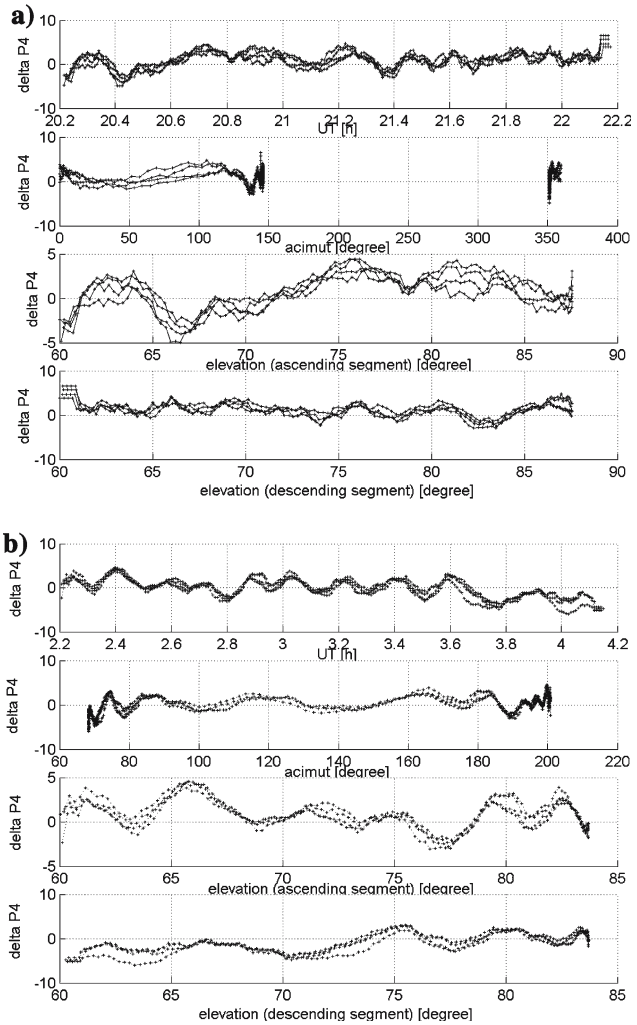

Fig. 4 Fingerprint of multi-path in the smoothed single differences in total electron content units (TECU) of the code-delay ionospheric against Universal Time (UT) for the first panel (the data point are corrected for the ∼4 min daily shift with respect to the first day), azimuth in the second panel and against elevation (ascending segment and descending segment) in the third and fourth panels. **a** Sites: lpgs and lpgB, PRN = 22, days = 188–191/05. **b** Sites: pots and potm, PRN = 08, days = 001–004/05

code-delay receiver IFB raging from 1.4 to 8.8 TECU were detected.

From the analysis presented in this contribution, we conclude that a proper model of the GPS-levelled code-delay ionospheric observable should include: (1) a term that does not cancel out when averaging over a continuous arc, associated with the multi-path effect and (2) the receiver code-delay IFB should be considered as a time-varying term. Further investigations should point to proper and effective way to estimate the effect of code-delay multi-path on each arc and experiment to assess the time scale and intensity of IFB variations made under controlled conditions.

Acknowledgements The authors are grateful to the reviewers, C. Mitchell, M. Crespi and S. Buchert for their helpful suggestions and comments on this paper. We would also like to thank the Editor-in-Chief, W. E. Featherstone, and Responsible Editor, G. Elgered, for their comments and editorial work on the paper.

References

Azpilicueta F, Brunini C, Radicella SM (2005) Global ionospheric maps from GPS observations using modip latitude. Adv Space Res JARS 7882:8. DOI 10.1016/j.asr.2005.07.069 (in press)

Bassiri S, Hajj A (1992) Higher order ionospheric effects on the Global Positioning System observables and means of modelling them. manuscripta geodaetica 18:280–290

Beutler G, Rotacher M, Schaer, Springer TA, Kouba J, Neilan RE (1999) The International GPS Service (IGS): an interdisciplinary service in support of Earth sciences. Adv Space Res 23(4):631–653. DOI 10.1016/S0273-1177(99)00160-X

Bishop G, Walsh D, Daly P, Mazzella A, Holland E (1994) Analysis of the temporal stability of GPS and GLONASS group delay correction terms seen in various sets of ionospheric delay data. In: Proceedings of the ION GPS-94, Salt Lake City, pp 1653–1661

Blewitt G (1990) An automatic editing algorithm for GPS data, Geophys Res Lett 17(3):199–202

Braasch M (1996) Multi-path effects. In: Parkinson BW Spilker JJ (eds) Global Positioning System: theory and applications, vol 1. Progress in astronautics and aeronautics, American Institute of Aeronautics and Astronautics, pp 547–568

Brunini C (1998) Global Ionospheric model from GPS measurements. PhD thesis, Facultad de Ciencias Astronómicas y Geofísicas, Universidad Nacional de La Plata, La Plata

Brunini C, van Zele MA, Meza A, Gende M (2003) Quiet and perturbed ionospheric representation according to the electron content from GPS signals. J Geophys Res 108:SIA4-1. CiteID 1056. DOI A2 10.1029/2002JA009346

Brunini C, Meza A, Azpilicueta F, van Zele A, Gende M, Diaz A (2004) A new ionosphere monitoring technology based on GPS. Astrophys Space Sci 290:415–429. DOI 10.1023/B:ASTR.0000032540.35594.64

Brunini C, Meza A, Bosch W (2005) Temporal and spatial variability of the bias between TOPEX- and GPS-derived total electron content. J Geod 79. DOI 10.1007/s00190-005-0448-z

Brunner FK, Gu M (1991) An improved model for the dual frequency ionospheric correction of GPS observations. manuscripta geodaetica 16:205–214

Byun SH, Hajj GA, Young LE (2002) Development and application of GPS signal multi-path simulator. Radio Sci 37(6):1098. DOI 10.1029/2001RS002549

Davies K, Hartmann GK (1997) Studying the ionosphere with the Global Positioning System. Radio Sci 32(4):1695–1703

Feltens J (1998) Chapman Profile Approach for 3-D Global TEC representation. In: Proceedings of the 1998 IGS Analysis Centres Workshop, Darmstadt, pp 285–297

Gao Y, Heroux P, Kouba J (1994) Estimation of GPS receiver and satellite L1/L2 signal delay biases using data from CACS. In: Proceedings of the KIS-94, Banff, pp 109–117

Gao Y, Lahaye F, Héroux P, Liao X, Beck N, Olynik M (2001) Modeling and estimation of C1-P1 bias in GPS receivers. J Geod 74(9):621–626. DOI 10.1007/s001900000117

Gaposchkin EM, Coster AJ (1993) GPS L1–L2 bias determination. Lincoln Laboratory Technical Report 971 (MIT), Massachusetts

Hernandez-Pajares M (2004) IGS Ionosphere WG: an overview. In: Proceedings of the COST 2004, Nice, pp 29–29

Hernández-Pajares M, Juan JM, Sanz J (1999) New approaches in global ionospheric determination using ground GPS data. J Atmos Solar Terr Phys 61:1237–1247

Jakowsky N, Sardon E, Egler E, Jungstand A, Klahn D (1996) About the use of GPS measurements for ionospheric studies. In: Beutler G, Hein GW, Melbourne WG, Seebr G (eds) GPS trends in precise terrestrial airborne and spaceborne applications. IAG Symposium vol 115. Springer, Berlin Heidelberg New York, pp 335–340

Langley R (1996) Propagation of the GPS signals. In: Kleusberg A, Teunissen P (eds) GPS for geodesy. Springer, Berlin Heidelberg New York, pp 103–140. ISBN 3-540-60785-4

Lanyi GE, Roth T (1988) A comparison of mapped and measured total ionospheric electron content using Global Positioning System and beacon satellite observations. Radio Sci 23:483–492

Leitinger R, Putz E (1988) Ionospheric refraction errors and observables. Atmospheric effects on geodetic space measurements. Monograph 12, School of Surveying, University of New South Wales, Sydney, pp 81–102

Ma XF, Maruyama T, Ma G (2005) Determination of GPS receiver differential biases by neuronal network parameter estimation method. Radio Sci 40:RS1002. DOI 10.1029/2004RS003072

Mannucci AJ, Wilson BD, Yuan DN, Ho CH, Lindqwister UJ, Runge TF (1998) A global mapping technique for GPS-derived ionospheric total electron content measurements. Radio Sci 33:565–582

Otsuka Y, Ogawa T, Saito A, Tsugawa T, Fukao S, Miyasaky S (2002) A new method for mapping of total electron content using GPS in Japan. Earth Planets Space 54:63–70

Sardon E, Zarraoa N (1997) Estimation of total electron-content using GPS data: how stable are the differential satellite and receiver instrumental biases? Radio Sci 32:1899–1910

Sardon E, Rius A, Zarraoa N (1994) Estimation of the transmitter and receiver differential biases and the ionospheric total electron content from Global Positioning System observations. Radio Sci 29:577–586

Schaer S (1999) Mapping and predicting the Earth's ionosphere using the Global Positioning System. PhD thesis, Astronomisches Institut, Universität Bern, Switzerland

Walter T, Blanch J, Rife J (2004) Treatment of biased error distributions in SBAS. J Global Position Syst 3(1–2):265–272